Coesite and stishovite in a shocked lunar meteorite, Asuka-881757, and impact events in lunar surface

E. Ohtani[a,1], S. Ozawa[a], M. Miyahara[a], Y. Ito[a], T. Mikouchi[b], M. Kimura[c], T. Arai[d], K. Sato[e], and K. Hiraga[e]

[a]Department of Earth Science, Graduate School of Science, Tohoku University, Sendai 980-8578, Japan; [b]Department of Earth and Planetary Science, University of Tokyo, Tokyo 113-0033, Japan; [c]Faculty of Science, Ibaraki University, Mito 310-8512, Japan; [d]Planetary Exploration Research Center, Chiba Institute of Technology, 2-17-1 Tsudanuma, Narashino, Chiba 275-0016, Japan; and [e]Institute for Materials Research, Tohoku University, Sendai 980-8577, Japan

Edited* by Ho-Kwang Mao, Carnegie Institution of Washington, Washington, DC, and approved November 22, 2010 (received for review June 30, 2010)

Microcrystals of coesite and stishovite were discovered as inclusions in amorphous silica grains in shocked melt pockets of a lunar meteorite Asuka-881757 by micro-Raman spectrometry, scanning electron microscopy, electron back-scatter diffraction, and transmission electron microscopy. These high-pressure polymorphs of SiO_2 in amorphous silica indicate that the meteorite experienced an equilibrium shock-pressure of at least 8–30 GPa. Secondary quartz grains are also observed in separate amorphous silica grains in the meteorite. The estimated age reported by the $^{39}Ar/^{40}Ar$ chronology indicates that the source basalt of this meteorite was impacted at 3,800 Ma ago, time of lunar cataclysm; i.e., the heavy bombardment in the lunar surface. Observation of coesite and stishovite formed in the lunar breccias suggests that high-pressure impact metamorphism and formation of high-pressure minerals are common phenomena in brecciated lunar surface altered by the heavy meteoritic bombardment.

moon | impact | collision

The lunar meteorites are unique samples, which provide information on the unexplored surface of the moon. The high-pressure polymorphs usually reported in impact craters of the Earth's surface have not been reported in lunar samples, and differences in impact conditions in the lunar surface have been suggested by previous workers; i.e., absence of high-pressure polymorphs of silica might be caused by volatilization during impact events in the high vacuum at the lunar surface (e.g., refs. 1 and 2). However, this is an unrealistic interpretation because volatilization during impact would require temperatures exceeding 1,700 °C. In addition, such volatilization would induce fractional sublimation of volatile elements like Na and K, for example, and much more importantly, isotopic mass-dependent fractionation of oxygen and magnesium. These features were never observed in shocked lunar samples. The lunar meteorites contain information on the shock events that were common in the early lunar surface. Asuka-881757 lunar meteorite was discovered in Antarctica, and was described by some authors (3, 4). This lunar meteorite is composed mainly of coarse aggregates of pyroxene, plagioclase (maskelynite), and ilmenite. It shows a variety of shock features such as the existence of maskelynite and glass matrix with compositions of mixtures of pyroxene and plagioclase that is clear evidence for melting of both plagioclase and pyroxene by shock and quenching of the melt mixture.

The difference in the age determined by ^{147}Sm-^{143}Nd and $^{39}Ar/^{40}Ar$ chronologies (5) indicates that the source basalt of this meteorite crystallized at 3,870 Ma and was impacted at 3,800 Ma, which is the time of the heavy bombardment on lunar surfaces. Therefore, the shock features recorded in this meteorite might provide information on conditions during the heavy meteoritic bombardment in the Moon. The cosmic-ray exposure age of this meteorite is one million years (6), which suggests that the meteorite was exposed in the space perhaps after launching from the lunar surface one million years ago, and the fragment was delivered to the Earth after this age. The detailed petrogenesis of this meteorite is given by Arai et al. (7).

We studied the shocked products of a lunar meteorite Asuka-881757 and discovered both coesite and stishovite crystallites in this meteorite based on the micro-Raman spectroscopic observations, scanning electron microscopy electron back-scatter diffraction (SEM-EBSD) measurements, and transmission electron microscopy (TEM) observations. We estimated the conditions of collision experienced by this lunar meteorite in the early moon based on its shock textures.

Results

We used a thin section of Asuka-881757 that contains various shock features such as maskelynite and glass. Asuka-881757 thin section is composed of three fragments, and we made detailed descriptions of two fragments Asuka-881757-2 and 881757-3. The back-scattered electron (BSE) images of the two fragments are given in Fig. 1.

Host and Shock-Induced Minerals. The fragments Asuka-881757-2 and 881757-3 contain large grains of pyroxene, maskelynite (originally plagioclase), ilmenite, glass perhaps formed by melting during the shock events, and small amorphous silica grains. The detailed descriptions of this meteorite were given in some papers (e.g., ref. 4).

Pyroxene grains are typically 1–2 mm in diameter showing elongated shapes toward *c* axis, and maskelynites are 1–5 mm in diameter. Pyroxene is highly fractured, whereas maskelynite shows chemical zonings from cores to rims ($An_{94-77}Or_{0-3}$). Symplectic intergrowths of silica-fayalite (Fo_{2-12})-hedenbergite are observed at the boundaries between pyroxene and maskelynite.

We observed small grains of amorphous silica, typically about 50–300 μm in diameter. An electron probe microanalyzer (EPMA) analysis showed that it contains Al_2O_3 in the range of 0.40–0.68 wt.% and Na_2O 0.08–0.14 wt.%. Raman spectra of the silica grains show no peaks but very broad peak suggesting that it is an amorphous silica phase. The SEM-EBSD analysis also shows no Kikuchi pattern, which is consistent with the Raman spectra.

Identification of Stishovite, Coesite, and Quartz in Amorphous Silica Grains. We observed several amorphous silica grains and found many small granular inclusions of coesite in the amorphous silica grains. Fig. 2*A* shows a transmitted microscopic image of a typical amorphous silica grain observed in the present lunar meteorite, a fragment Asuka-881757-3. Many coesite inclusions with a grain

GEOLOGY

Author contributions: E.O. and T.A. designed research; E.O., S.O., and M.M. performed research; S.O., M.M., Y.I., T.M., M.K., K.S., and K.H. contributed new reagents/analytic tools; E.O., S.O., and M.M. analyzed data; and E.O. wrote the paper.

The authors declare no conflict of interest.

*This Direct Submission article had a prearranged editor.

Freely available online through the PNAS open access option.

[1]To whom correspondence should be addresed. E-mail: ohtani@m.tohoku.ac.jp.

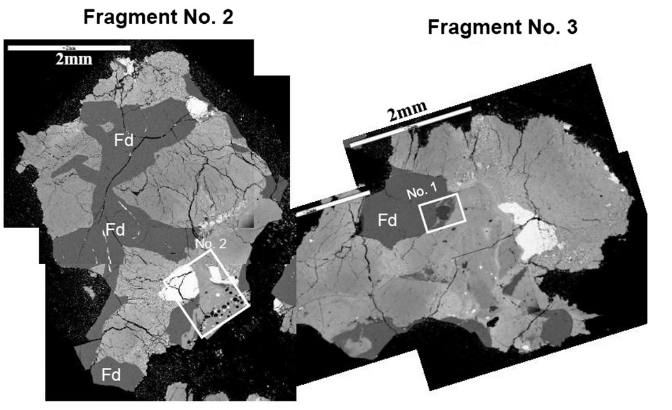

Fig. 1. The BSE images of Asuka-881757 lunar meteorites. Two fragments, Asuka-881757-2 and 881757-3 were studied in this work. The amorphous silica grain, No. 1, in a white box, contains coesite and stishovite inclusions. Another silica grain, No. 2, contains quartz inclusions.

size of 1–10 μm were identified in the amorphous silica grains by the micro-Raman spectroscopy (Fig. 2*A*, *Inset*) and SEM-EBSD analysis.

We applied the SEM-EBSD analysis and measured the Kikuchi patterns of the inclusions, which are given in Fig. 3*A*. The Kikuchi patterns shown in this figure were clearly explained by the crystal structure of coesite. The Kikuchi patterns of the adjacent grains shown in crystals 1, and 2 in Fig. 3*A* indicate that the granular coesite crystals in the adjacent area (typically in an area of about 30 μm × 30 μm) show a common crystallographic orientation suggesting that they are parts of the same crystal.

We also conducted TEM observation of the amorphous silica grain containing coesite crystallites (Figs 2*A* and 3*A*), and confirmed existence of both stishovite and coesite crystals as shown in Fig. 4 *A* and *B*. These photomicrographs show that microcrystals of coesite have a rounded shape with a grain size of 300 nm, whereas those of stishovite have an angular shape with a size of 100 nm. Such morphology of stishovite indicates that it did not crystallize from a melt. Otherwise it should have occurred as acicular crystals or needles.

An amorphous silica grain in a lunar meteorite fragment Asuka-881757-2 and its high magnification image are given in Fig. 2*B*. We identified quartz inclusions in the amorphous silica grains with the grain size of 1–10 μm in this fragment (Figs. 1 and 2*B*) by the Raman spectroscopy and SEM-EBSD analysis. Fig. 3*B* shows the Kikuchi patterns of quartz determined by the SEM-EBSD measurement of the inclusions. The Kikuchi patterns indicate that the inclusions are quartz and the adjacent crystals in an amorphous silica grain show a common crystallographic orientation as shown in this figure. We observed the Raman peak of the quartz inclusions at 464 cm^{-1}, which is at higher wave number than that of the shocked quartz observed at 456 cm^{-1} (8), thus strongly suggesting that this quartz originated from partial back transformation of stishovite and/or coesite.

Discussion

The amorphous silica grains containing coesite, stishovite, and quartz inclusions might have been originally cristoballite formed in the final stage of crystallization of the host basaltic magma (1). Original plagioclase crystals are converted to maskelynite in this sample. We observed a heterogeneous quench glass formed by partial melting of both maskelynite and pyroxene and clear evidence for mixing of the two melts as shown in Fig. 2*B*. The clear boundary between the amorphous silica grains and the quenched pyroxene-feldspar glasses indicates that amorphous silica grains were not molten during the high temperature stage of the formation of the glasses. The spherical holes observed in Fig. 2*B* may be formed by vesiculation or originally filled by

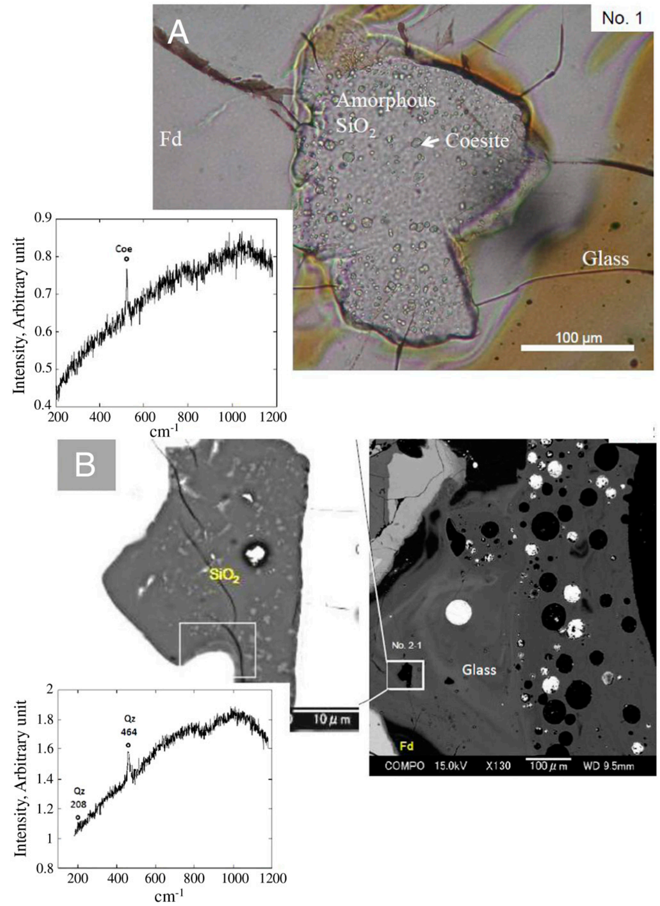

Fig. 2. Amorphous silica grains No. 1 in the fragments, Asuka-881757-2 and 881757-3. (*A*) Amorphous silica grain, No. 1 contains many coesite inclusions with 1–10 μm in diameter. A Raman spectrum of an inclusion is shown in the *Inset* of this figure, showing the typical Raman peak of coesite at 522 cm^{-1}. Fd, maskelynite with a feldspar composition; Glass, glass showing mixing of two melts with the pyroxene (brown color) and feldspar (gray) compositions. (*B*) a BSE image of amorphous silica grain No. 2. Inclusions of quartz were observed in this silica grain. SiO_2, amorphous silica; A Raman spectrum of an inclusion is shown in the inset of this figure, showing the Raman peaks of quartz at 208 cm^{-1} and 464 cm^{-1}. The major Raman peak observed at 464 cm^{-1} is larger than 456 cm^{-1} that is typical for the shock compressed quartz (8), suggesting that the quartz grains were formed by the back transformation from high-pressure phases.

iron-sulfide spheres and removed during polishing. In the former case, the vesicles indicate that melting of the meteorite took place at ambient pressure.

This is a set of high-pressure polymorphs in lunar meteorites, such as stishovite and coesite, in addition to quartz with characteristic textures, although we also reported coesite from a CB chondrite (9). We observed small crystallites of stishovite with a grain size of ∼100 nm in amorphous silica by TEM (Fig. 4*B*). Existence of stishovite crystallites in amorphous silica indicates that the peak pressure of the shock compression of the lunar meteorite was at least 8 GPa (10) and it could have been higher than 30 GPa due to very low concentrations of Al_2O_3 (11). No occurrence of α-PbO_2 type SiO_2, seifertite indicates that the pressure was lower than ∼35 GPa (12). The amorphous silica might be formed by conversion from former high-pressure polymorphs such as stishovite. According to previous studies (13), the shock-induced silica glass shows a characteristic defect band at about 602 cm^{-1}, and its intensity decreases by annealing at high temperatures. Our Raman spectra measurements of the amorphous silica containing coesite and stishovite show no such Raman band corresponding to shocked signature, suggesting

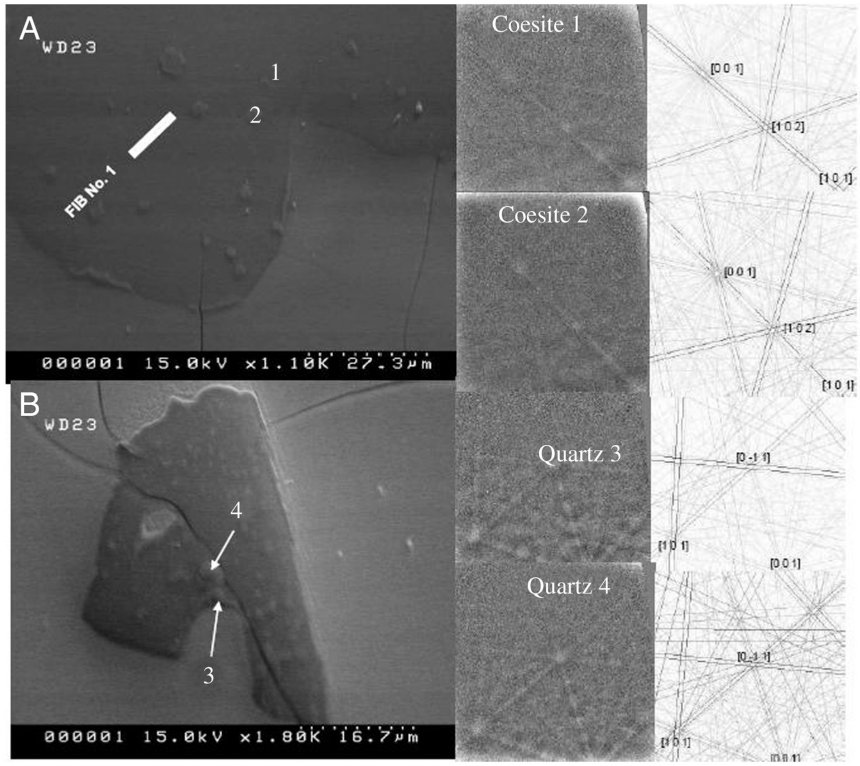

Fig. 3. Secondary electron images of amorphous silica grain. (*A*) Amorphous silica grain, No. 1. The Kikuchi patterns of the two coesite grains, 1, and 2 are given in this figure. Two adjacent grains show a similar crystallographic orientation. FIB No. 1 indicates the slice prepared by FIB for TEM observation (see text and Fig. 4). (*B*) Amorphous silica grain, No. 2. The Kikuchi patterns of the grains 3 and 4 indicate that the two grains are quartz.

formation of the amorphous silica by back transformation from high-pressure polymorphs. The existence of stishovite and seiferetite was also reported previously in a lunar meteorite based on the cathodoluminescence studies alone (14), although detailed description of their occurrence has not been provided, suggesting that impact in the lunar surface may be exceeding the stability field of stishovite; i.e. >30 GPa. The other high-pressure phases such as wadsleyite and ringwoodite were reported previously (15) although their occurrences were not described in detail. Existence of these minerals is consistent with the shock pressure estimated here.

The preferred orientation of coesite and quartz crystals observed by the SEM-EBSD measurement (Fig. 3 *A* and *B*) suggests that they are formed by topotactic relations with the preexisting crystals such as stishovite. The major Raman peak of quartz at 464 cm^{-1} of in the amorphous silica indicates that it was not formed by the shock compression but was formed by the back transformation during decompression (8), which is consistent with the preferred orientation of the crystals in the amorphous silica.

The dating of this meteorite was made by Misawa et al. (5), and suggested that the crystallization age is $3871 + 57$ Ma, which was conducted by the ^{147}Sm-^{143}Nd dating, whereas the impact age is $3798 + 12$ Ma dated by the $^{39}Ar/^{40}Ar$ chronology. The $^{39}Ar/^{40}Ar$ dating that can be modified easily by the shock events was made separately both for shocked glass and maskelynite in this meteorite, and the dates were reported to be $3790+16$ Ma, $3808 + 18$ Ma respectively (5). The similar ages for the two parts of this meteorite strongly suggest these parts were shocked by a similar collision. The mean age of the glass and the maskelynite, $3798 + 12$ Ma by the $^{39}Ar/^{40}Ar$ chronology is considered to be the age of formation of the glass and maskelynite reset by a large shock event in the lunar surface. Because no $^{39}Ar/^{40}Ar$ ages younger than this age were measured in this meteorite, coesite and stishovite in amorphous silica grains in the shock-induced glass are considered to be the products of this collision occurred in the early lunar surface $3798 + 12$ Ma ago,

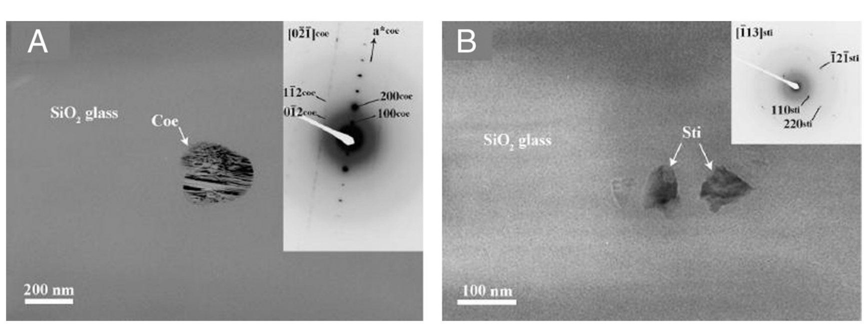

Fig. 4. TEM images. (*A*) A coesite nano-crystal observed in the amorphous silica grain recovered from the sample No. 1. The slice was recovered from FIB No. 1 of the sample in Fig. 3*A* (*Upper*). A SEAD pattern clearly indicates coesite. Coe, coesite. (*B*) Stishovite crystals observed in the same slice, FIB No. 1. A SEAD pattern indicates existence of stishovite. Sti, stishovite.

and we can safely exclude a possibility of formation of these high-pressure polymorphs by the shock event that launched this meteorite from the lunar surface in a later stage. We can also exclude the possibility that these minerals formed at the impact on the Earth's surface. Because a shock vein was cut by fusion crust, the formation of shock vein and high-pressure minerals evidently predated the atmospheric entry (16).

The shock-induced high-pressure minerals in lunar samples have been so far ignored as important mineral constituents in lunar surface regolith breccias experienced by heavy collisions during the early lunar history (1, 2). The present occurrence of several polymorphs of silica such as coesite, stishovite, and quartz in amorphous silica grains suggests that high-pressure minerals might be common constituent minerals in lunar surface. The high-pressure silica assemblage and the evidence for partial back transformation of one or both of them to secondary quartz allowed to uncover the phase transformations both during the dynamic compression and the decompression stages. We emphasize that further studies on high-pressure polymorphs in lunar regolith may be needed by using advanced microanalyses.

Experimental Methods

We identified primary, shock-induced, and secondary minerals and documented their spatial distributions in this meteorite by using the micro-Raman spectroscopy. We also used an optical microscope, SEM, and TEM to identify the shock texture in this meteorite. Raman spectra of the constituent minerals in the meteorite were measured by the JASCO NRS-2000 micro-Raman spectrometer with a nitrogen-cooled CCD detector at Tohoku University. A microscope was used to focus the excitation laser beam (514.5 nm lines of a Princeton Instruments Ar^+ laser). The sample was excited by the laser power of 8–12 mW for collecting the Raman spectra. The size of the laser beam was 1 μm in diameter. The crystalline nature of minerals and their crystallographic orientations were investigated by Thermo Noran Phase ID EBSD system installed into the Hitachi S-4500 field emission (FE)-SEM at the University of Tokyo. The accelerating voltage of the incident beam was 15 kV, and the beam current was 2–3 nA. Calculations of Kikuchi patterns and analyses of the observed patterns were performed using a program by Kogure (17). Mikouchi et al. (18) reported the detailed analytical conditions for EBSD used in this work.

The distribution and textures of the high-pressure minerals were investigated by optical microscope and an FE-SEM, JEOL JSM-71010, at Tohoku University in Sendai, Japan. Accelerating voltage and electron-beam current are 15 kV and ∼1 nA, respectively. The chemical compositions of minerals were determined by the electron probe microanalyzer (EPMA; JEOLJXA-8800M superprobe). Analyses were acquired using a 15 kV acceleration voltage and a 5–15 nA beam current. The electron beam was focused to less than 1–10 μm. A dedicated liquid-N_2 cooling sample stage was employed for amorphous silica, maskelynite, and glass to reduce electron-beam damage.

Slices of the sample for TEM observations were prepared by the focused ion beam (FIB) system, JEOL JEM-9320FIB and FEI Quanta 3D. A gallium ion beam was accelerated to 30 kV during the sputtering of the slices. The slices were ∼100 nm in thickness. A JEOL JEM-2010 transmission electron microscope operating at 200 kV was employed for conventional TEM and selected area electron diffraction.

ACKNOWLEDGMENTS. This work was supported by Japan Society for the Promotion of Science Grants (E.O. and S.O.), and conducted as a part of Global Center for Excellence program for Earth and Planetary Sciences, Tohoku University. A part of this work was supported by the "Nanotechnology Support Project" of the Ministry of Education, Culture, Sports, Science, and Technology (MEXT), Japan.

1. Papike JJ (1998) Comparative planetary mineralogy: Chemistry of melt-derived pyroxene, feldspar, and olivine. In Planetary Materials. *Reviews in Mineralogy & Geochemistry*, ed JJ Papike (Mineralogical Society of America, VA), 36, pp 7-1–7-11.
2. Lucey P, et al. (2006) Understanding the lunar surface and space-moon interactions. In New Views of the Moon. *Review in Mineralogy & Geochemistry*, eds L Bradley et al. (Mineralogical Society of America, VA), 60, pp 83–220.
3. Koeberl C, Kurat G, Brandstätter F (1993) Gabbroic lunar mare meteorites Asuka-881757 (Asuka-31) and Yamato 793169: Geochemical and mineralogical study. *Proc NIPR Symp Antact Meteorites* 6:14–34.
4. Arai T, Takeda H, Warren PH (1996) Four lunar meteorites: Crystallization trends of pyroxenes and spinels. *Meteorit Planet Sci* 31:877–892.
5. Misawa K, Tatsumoto M, Dalrymple GB, Yanai K (1993) An extremely low U/Pb source in the Moon: U-Th-Pb, Sm-Nd, Rb-Sr, and $^{40Ar/39}$Ar isotopic systematics and age of lunar meteorite Asuka 881757. *Geochim Cosmochim Acta* 57:4687–4702.
6. Nishiizumi K, Arnold JR, Caffee MW, Finkel RC, Southon J (1992) Cosmic ray exposure histories of lunar meteorites Asuka 881757, Yamato 793169, and Calcalong Creek. *17th Symp Antarct Meteorites* pp 129–132.
7. Arai T, et al. (2010) Antarctic lunar meteorites Yamato-793169, Asuka-881757, MIL 05035, and MET 01210 (YAMM): Launch pairing and possible cryptomare origin. *Geochim Cosmochim Acta* 74:2231–2248.
8. El Goresy A, Gillet P, Chen M, Stähle V, Graup G (2001) In situ finding of the fabric stettings of shock-induced quartz/coesite phase transition in crystalline clasts in suevite of the Ries crater, Germany. *Meteorit Planet Sci* 36(Supplement):A69–A70.
9. Weisberg MK, Kimura M, Suzuki A, Ohtani E, Sugiura N (2006) Discovery of coesite and significance of high pressure phases inthe Gujba CB chondrite. *Lunar Planet Sci* 37:1788.
10. Akimoto S, Yagi T, Inoue K (1977) High temperature-pressure phase boundaries in silicate systems using in situ X-ray diffraction, in high-pressure research: Applications in geophysics . (Academic, New York), pp 595–602.
11. Lakshtanov LD, et al. (2007) The post-stishovite phase transition in hydrous alumina-bearing SiO_2 in the lower mantle of the earth. *Proc Natl Acad Sci USA* 104:13588–13590.
12. El Goresy A, et al. (2008) Seifertite, a dense orthorhombic polymorph of silica from the Martian meteorites Shergotty and Zagami. *Eur J Mineral* 20:523–528.
13. Okuno M, Reynard B, Shimada Y, Syono Y, Williame C (1999) A Raman spectroscopic study of shock-wave densification of vitrious silica. *Phys Chem Miner* 26:304–311.
14. Channaoui-Auddjehane H, Jambon A (2008) First evidence of high pressure silica: Stishovite and seifertite in lunar meteorite Northwest Africa 4734. *Meteorit Planet Sci* 43(Supplement):A32.
15. Barrat JA, et al. (2005) Lithium behavior during cooling of a dry basalt: An ion-microprobe study of the lunar meteorite Northwest Africa 479 (NWA 479). *Geochim Cosmochim Acta* 69:5597–5609.
16. Kimura M, Chen M, Yoshida T, El Goresy A, Ohtani E (2004) Back-transformation of high-pressure phases in a shock melt vein of an H-chondrite during atmospheric passage: Implications for the survival of high-pressure phases after decompression. *Earth Planet Sc Lett* 217:141–150.
17. Kogure T (2003) A program to assist Kikuchi pattern analysis. *J Crystal Soc Jpn* 45:391–395 (Translated from Japanese).
18. Mikouchi T, et al. (2009) Dmitryivanovite: A new high-pressure calcium aluminum oxide from the Northwest Africa CH3 chondrite characterized using electron back-scatter diffraction analysis. *Am Mineral* 94:746–750.